GRATING OPTIC FIBER SENSORS DETECTION OF SMART POLYMER COMPOSITE DELAMINATION

Dan SAVASTRU[1], Marina TAUTAN[2], Valeriu SAVU[3], Madalin Ion RUSU[4*], Alexandru STANCIU[5]

The paper presents the results obtained in simulation of a Smart Composite Polymer Material (SCPM) interfacial failure or delamination detection using a Long Period Grating Fiber Sensor (LPGFS) embedded into polymer matrix and operated directly in a simple transmission setup. The SCPM delamination is analyzed using a FEM based cohesive zone model (CZM). The modification of the LPGFS transmission spectrum induced as a delamination collateral effect are observed and used for delamination detection. The paper is pointing to an improved simulation/design method of smart composite polymer materials and their applications in various fields such as aeronautics, industry, medicine and defense.

Keywords: smart composite polymer material, composite delamination, optical fiber composite delamination sensor, Long Period Grating Fiber Sensor

1. Introduction

Polymer composite materials have multiple applications in aerospace activities, as parts of aircrafts, in chemical industry and in agriculture, as pipes and other parts of complex systems, in research domain for device construction, in medicine, as construction parts of various devices. In all these kinds of applications the failure of composite manufactured parts caused by interfacial failure or delamination is an important issue for the solution of which important research efforts are made in order to improve polymer composite material reliability and the design of reliable mechanical parts made of these materials [1-14]. A large part of these research efforts is related to the delamination detection as the initial stage of the process. In the paper there is analyzed the possibility of using long period grating fiber sensor (LPGFS) embedded into polymer matrix of composite material for delamination detection [10-24]. The investigation of polymer composite delamination is based on the assumption that applied mechanical loads induce relative displacements of composite material parts which are converted into internal

[1] Eng., National Institute of R&D for Optoelectronics INOE 2000, Romania, e-mail: dsavas@inoe.ro
[2] Eng., National Institute of R&D for Optoelectronics INOE 2000, Romania, e-mail: marina@inoe.ro
[3] Eng., National Institute of R&D for Optoelectronics INOE 2000, Romania, e-mail: savuv@inoe.ro
[4]* Corresponding author - Eng., National Institute of R&D for Optoelectronics INOE 2000, Romania, e-mail: madalin@inoe.ro
[5] Eng., National Institute of R&D for Optoelectronics INOE 2000, Romania, e-mail: alexandru.stanciu@inoe.ro

strains detected by LPGFS [23-26]. The optical signal generated by the LPGFS can be used as input into a feedback loop of an automatization device integrated to the composite material part, the composite material being transformed into a "smart" one (SCPM). The main purpose of the paper consists of presenting simulation results obtained using a finite element method (FEM) analysis applied to the polymer matrix of composite material for calculation of strain induced into a SCPM by the delamination and simulation of how this strain is affecting a LPGFS embedded in the polymer matrix of the composite. For the LPGFS there is investigated the transmission spectrum consisting of absorption bands as the long period grating (LPG) effect when the host optic fiber is placed in air, this being the "zero/reference state" and when it is embedded into composite polymer matrix, the absorption bands being shifted as compared to the "zero state". The delamination induced strain affecting the optic fiber can be observed by the absorption bands spectral shifts and broadening. These observed absorption bands spectral shift and broadening are the measure of the induced strains and of the delamination effect. There were analyzed the LPG version of the grating optic fiber sensor, the LPG being preferred because of its possible use for detection of polymer matrix chemical alteration. The investigated LPGs are inscribed into a single mode (SM) optic fiber by various methods which are briefly characterized. The composite delamination process is analyzed using the cohesive zone model (CZM). CZM implies the traction-separation law that describes the softening in the cohesive zone near the delamination point/zone. In the performed analysis a bilinear traction-separation law in a laminated composite using the layered shell interface (LSI) was used for description of mixed-mode softening and delamination propagation. The simulations were performed considering a composite material plate of 1.5 mm thickness with PVC or PDMS matrix. The grating optic fiber sensor is analyzed as embedded in the polymer matrix being used as stress detector.

2. Theory

Delamination of laminate polymer composite materials is a complex process. One possibility to analyze the delamination process is to consider the strain producing it as the summation of different types of strain induced by primary sources of mechanical stress [1-14]. In Figure 1 there are schematically presented four primary modes of mechanical stress inducing strain into the investigated laminate polymer composite materials, each corresponding to internal relative displacement of composite material components, i.e., the polymer matrix and the foils [1-14].

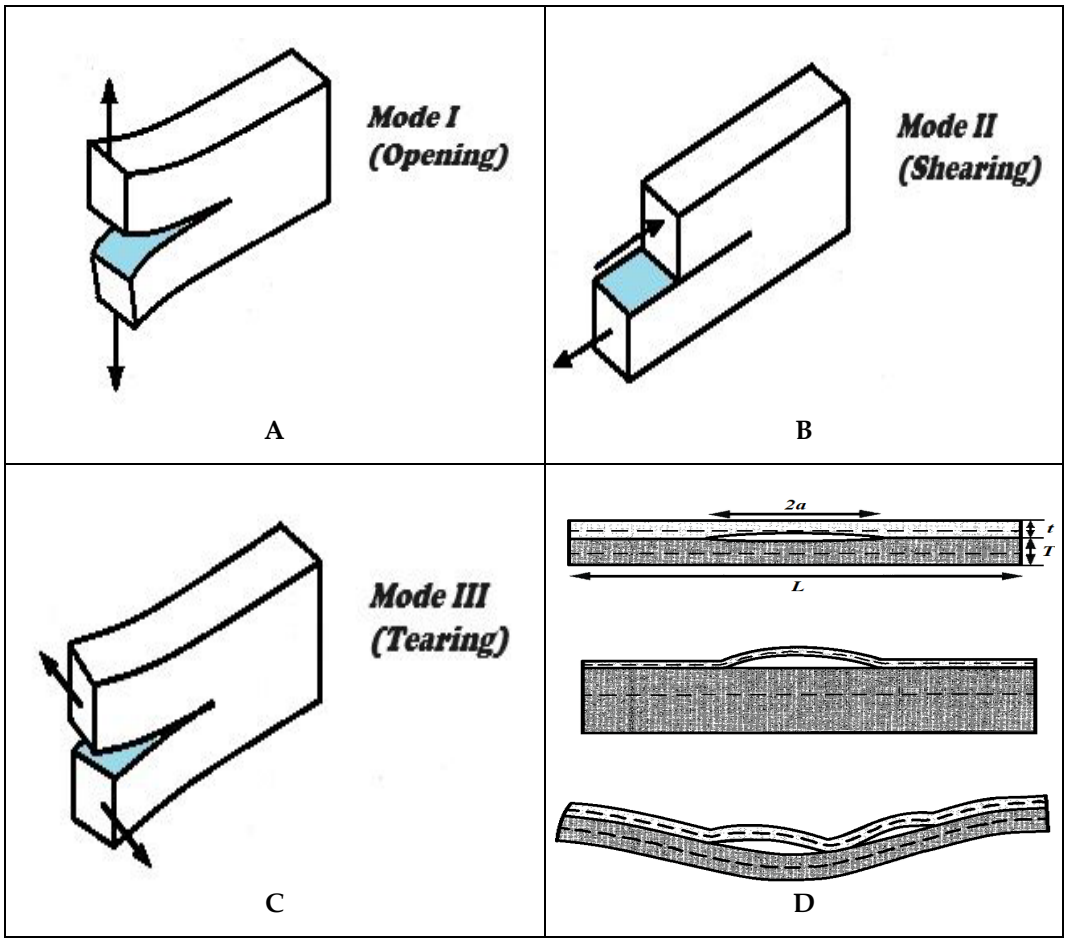

Fig. 1. Schematically representation of four primary modes of mechanical stress induced strain into the investigated laminate polymer composite materials. A- Delamination of laminate polymer composite materials Mode I – Opening; B- Delamination of laminate polymer composite materials Mode II – Shearing; C- Delamination of laminate polymer composite materials Mode III – Tearing; D- Delamination of laminate polymer composite materials Mode IV - Buckling.[27]

CZM is gathering the four primary delamination modes of mechanical stress, Opening, Shearing, Tearing and Buckling. One main assumption of the study is that the four primary delamination modes induce internal strain into polymer matrix of composite material. The induced delamination strain has effects on the LPGFS embedded into polymer matrix, this being the induced strain detection. The four primary delamination modes induced strain in LPGFS zone is transformed into elongation/contraction and/or bending of the optic fiber. The LPGFS is embedded into the epoxy resin layer has the capacity to sense the delamination initiation and propagation into the composite, the detachment of the two layers from the epoxy resin matrix of composite.

Fig. 2 shows schematic representation of the system investigated during the simulation. A composite plate made of two layers each of 1.5 mm thickness suffers a delamination process. The composite plate has the dimensions 50 mm × 75 mm. In Fig. 2 there can be observed the interfacial failure or delamination process using CZM marked with yellow. The delamination initiation and propagation into the investigated composite plate can be noticed. In Fig. 2 the detachment of the two layers from the epoxy resin matrix can be observed. The LPGFS is embedded into the epoxy resin layer.

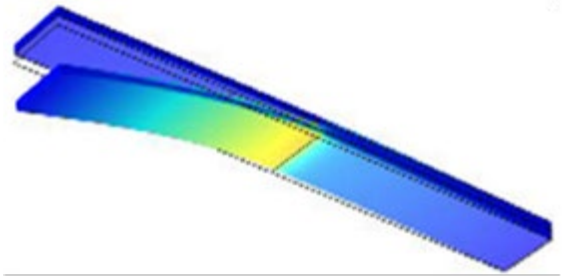

Fig. 2. Schematic representation of the investigated system.

LPGFS have characteristics which make it of interest for various applications such as small volume intrinsic optical fiber devices, immunity to electromagnetic interference because of their dielectric (non-conducting) structure, low-level back reflection and low insertion losses, as well as being relatively insensitive to polarization effects [17-28]. Because of these characteristics, in the investigation performed, the LPGFS is used as a delamination detector. The main part of LPGFS is constituted by a long period grating (LPG) induced into a Single Mode (SM) optic fiber. The LPG is constituted by a modulation of the refractive index of the optical fiber core by either inducing a physical deformation, a repeated slight tapering in the optical fiber material using low power CO2 laser thermal processing or by modifying its value ex using UV laser point-by-point focusing [17-24]. The second technique is more expensive and the LPG is usually formed in photosensitive optical fiber core by creating increased concentrations of color center point defects induced by exposing the core material to ultraviolet (UV) typically in the 242 nm to 248 nm wavelength range laser light [18-22]. The second technique has a main drawback of the LPG manufactured using this technology is that the color centers are thermally instable from temperatures greater than 250-300°C [23-28]. The LPG obtained using the first technique are operable at temperatures higher than 300°C [23-28].

LPGFS operation is described by the Eq. (1) for which there is no analytical solution:

$$\lambda_l^{(i)} = \left(n_{eff}\left(\lambda^{(i)}\right) - n_{clad}^{(l)}\left(\lambda^{(i)}\right)\right)\Lambda_{LPG} \quad (1)$$

In Eq. (1) $\lambda^{(i)}$ is the wavelength of the light signal injected in the core of the SM optic fiber, $n_{eff}\left(\lambda^{(i)}\right)$ is the effective value of the core refraction index, $n_{clad}^{(k)}\left(\lambda^{(i)}\right)$ is the refractive index effective value corresponding to the possible light cladding co-propagating mode l and Λ_{LPG} is the grating spatial period modulation. It is worth to underline that $\lambda_l^{(i)}$ in Eq. (1) denotes the Bragg resonance wavelength value [17-30]. For each $\lambda^{(i)}$ there can be calculated a coupling coefficient between the core mode and the kth cladding mode, κ_i, using $\lambda_l^{(i)}$ value, the grating modulation period and amplitude values [17-30]. κ_i represents a measure of the energy transfer from core mode to the lth co-propagating cladding mode when the light signal propagating through optic fiber core is incident on LPG. At macroscale, this energy transfer with maxima at Bragg resonance wavelength can be observed as absorptions bands in the optic fiber transmission spectrum. Any modification of LPGFS ambient represents a variation of its refractive index which is converted into spectral shifts of absorptions bands in the optic fiber transmission spectrum. Using Eq. (1), there can be calculated the grating characteristic Phase Matching Curves (PMC). PMC are parametric curves defined by the of pairs consisting of Λ_{LPG} (grating modulation period) and $\lambda_l^{(i)}$ (Bragg resonance wavelength). In Eq. (1), the core and cladding refractive index effective values are both functions of the investigated optic fiber mechanical characteristics which are dependent on applied stresses which induce strains equivalent to twisting and/or bending the SCPM, practically the LPGFS ambient. Finally, the SCPM twisting and/or bending means strain created in the system which is equivalent to spectral shifts of the LPG absorption peaks and broadening of the corresponding bands.

3. Simulation Results

The optical fiber sensor system used for delamination detection was investigated in three main steps. Without reduction of the analysis generality, the simulations were performed on a grating with a length of 50 mm, an amplitude of core refraction index modulation amplitude δn_{co} of 2×10^{-4} and a visibility of 1. The investigated LPGFS was embedded in the PDMS or PLA polymer matrix of a composite material. During simulations the PDMS refractive index is 1.4303, a value lower than that of the optic fiber cladding. The first step consists of n_{eff} and

$n_{clad}^{(i)}$ calculation. In the second step the PMC are simulated and the Bragg resonance wavelengths $\lambda^{(i)}$ and the mode coupling coefficients κ_i are calculated. The Bragg resonance wavelengths $\lambda^{(i)}$ are calculated analytically using a method which can be imaged graphically: in Figure 3, where PMC are represented in a $(\lambda^{(i)}, \Lambda_{LPG})$ coordinates system, with ΛLPG denoting the grating period, draw a line parallel to ΛLPG axis located at a given $\lambda^{(i)}$, the intersection points of this line with the Phase Matching Curves are the Bragg resonance wavelengths corresponding to the absorption peaks in the optic fiber transmission spectrum. In Figure 3, there are represented PMC calculated for first 9 possible co-propagating cladding modes, the modes for which κ_i have significant values. In Figure 3 there is represented a practical situation: the "given $\lambda^{(i)}$" is chosen to be in the middle of an Interrogation Monitor entrance spectral domain 1510 - 1595 nm and to correspond to a Λ_{LPG} of 775 μm, a possible value of grating period. For the investigated system, the chosen grating period was of 775 μm. For the investigated system, the copropagating mode having the calculated parameters is denoted as Mode 6 with Bragg resonance wavelength λ_{res} = 1541.93 nm. The investigated LPGFS operation as a detector is accomplished by observing the spectral shifts of λ_{res} versus ambient refractive index variation. In Figure 3 the results obtained in simulation of PMC for the investigated LPGFS are presented. In Figure 3 it can be noticed that a second auxiliary line, this time corresponding to Λ_{LPG} of 775 μm and parallel to wavelength axis intersects the Phase Matching Curves representing Modes 1 to 7 in seven different points, each corresponding to a mode. These intersection points correspond each to a $\lambda_l^{(i)}$ value. There are kept only these first seven Modes because higher ones correspond to $\lambda^{(i)}$ situated outside the spectral range of interest. Because of a higher accuracy, the simulations were accomplished using an analytical method of $\lambda^{(i)}$ calculation instead of a graphical one.

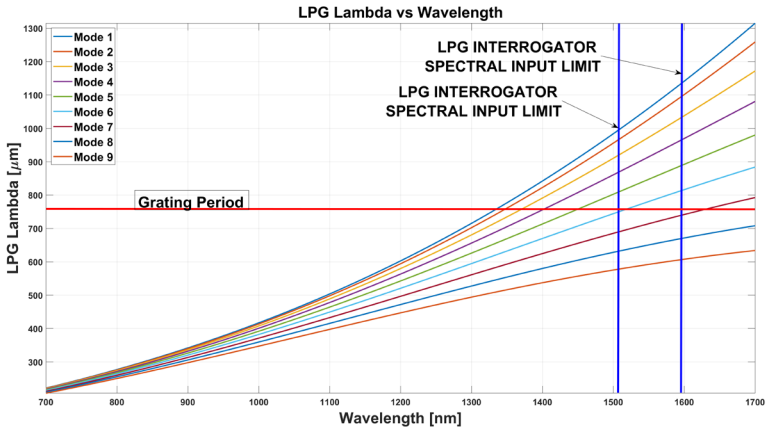

Fig. 3. Phase Matching Curves obtained for LPGFS embedded in PLA.

An important step in LPGFS investigation consists of its transmission spectrum simulation. In Fig. 4, there are presented the results obtained for the investigated system in the case of a grating with 775 μm modulation period. It can be observed in Figure 4 that the absorption Bragg resonance bands have decreasing intensities regarding resonance wavelength because the modes having longer resonance wavelength, corresponding to lower photon energy for which the Bragg resonance condition is easier accomplished corresponding to the cladding modes which co-propagate with the core fundamental mode closer to the optic fiber axis. Extracted from LPGFS transmission spectrum, in Figure 5 there is presented the simulated transmission spectrum of Mode 6 which has a 4.25 nm Full Width Half-Measure (FWHM) of and an amplitude of -9.48 dB.

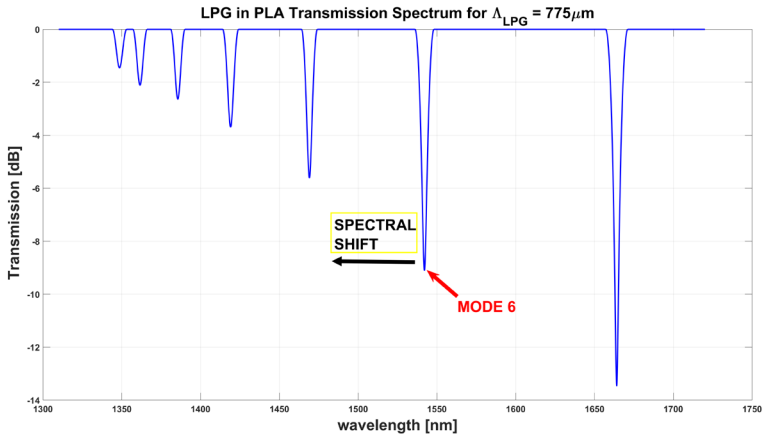

Fig. 4. The simulated transmission spectrum of the investigated LPGFS.

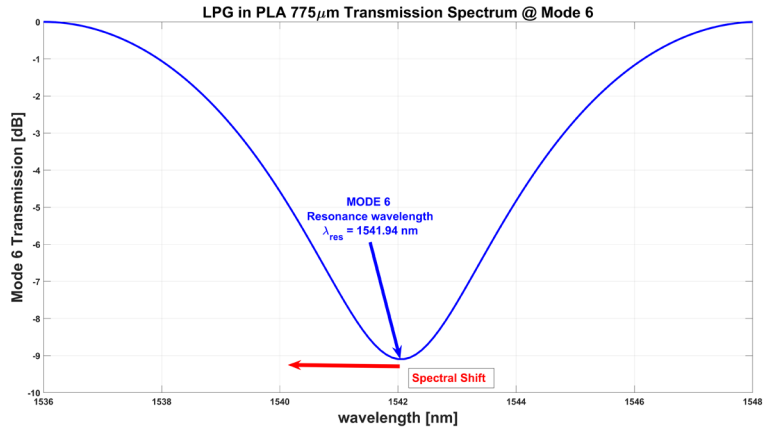

Fig. 5. The simulated transmission spectrum of Mode 6.

In Fig. 6 there is represented the buckling delamination process in the first stages. The red arrows mark the LPGFS input and output connections. The LPGFS is embedded in the polymer matrix of the composite. In Figure 6 there are represented two zones of applying forces causing delamination. It can be observed that at the LPGFS level, the buckling delamination process is equivalent to an optic fiber bending. The delamination process is causing the strain in the LPGFS immediate ambient. In Fig. 7 there are presented the results obtained in simulation of Bragg resonance wavelength spectral shift induced by composite strains. The simulation and experimental results are in an acceptable agreement. The delamination is caused by bending the investigated plate. The use of LPGFS is analyzed by considering the strain induced by bending.

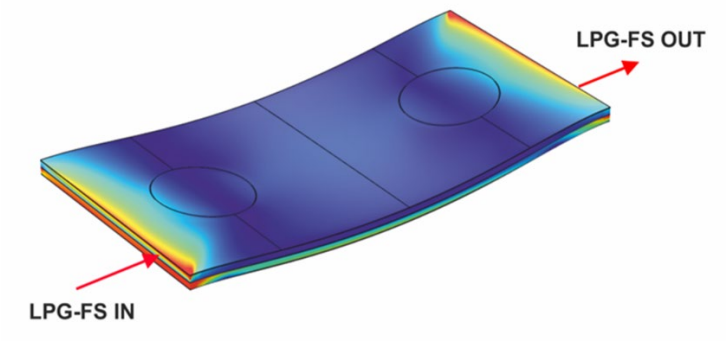

Fig. 6. Schematic representation of the investigated system induced strains.

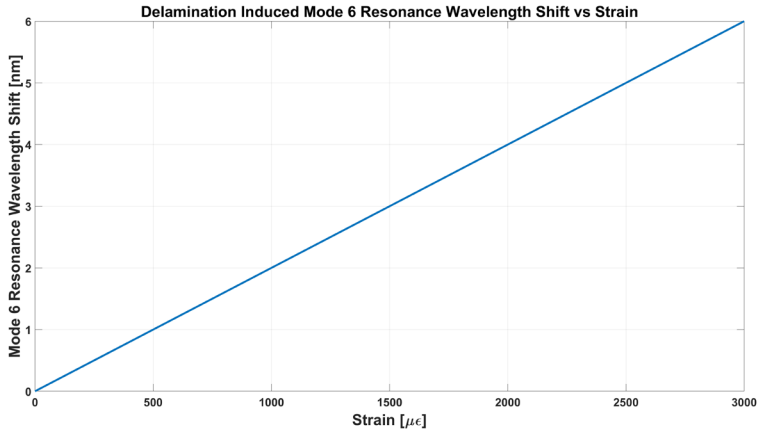

Fig. 7. The Mode 6 Resonance Wavelength Shift versus strain induced by delamination.

In Fig. 7 there is presented the simulated LPGFS Mode 6 λ_{res} spectral shift variation caused by the delamination stress of the investigated system. A quite

linear spectral shift for the applied stress can be noticed, enabling an accurate determination of the stress.

In Fig. 8 the investigated system regarding the interface health is presented. The two zones of applying forces causing delamination can be noticed. The delamination is caused by bending the investigated plate. Notice that the LPGS is mounted between the two layers. The red arrows mark the LPGFS input and output connections. The use of LPGFS is analyzed by considering the strain induced by bending.

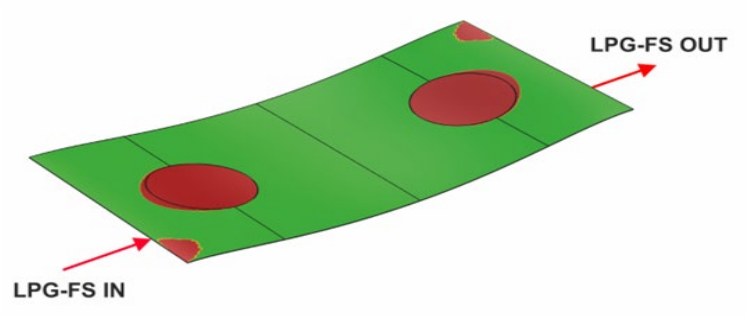

Fig. 8. Schematic representation of interface health of the investigated system.

In Fig. 9 the variation of the LPGFS Mode 6 λ_{res} spectral shift versus strain induced by the interface health is presented. It was considered only the interface contribution. A quite linear spectral shift for the applied strain can be noticed, enabling an accurate determination of the strain.

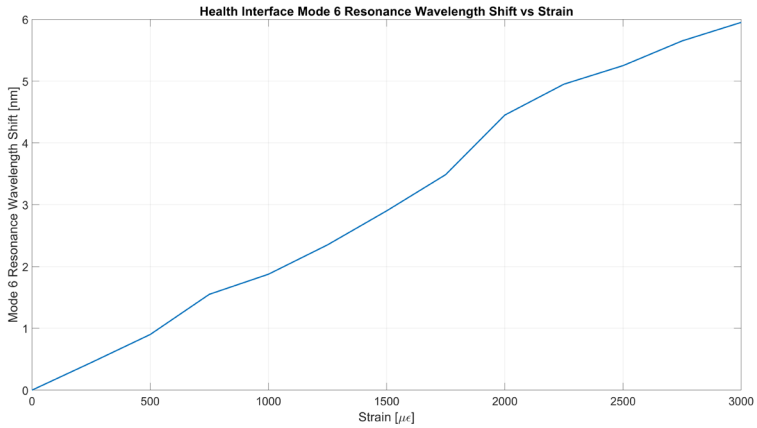

Fig. 9. The simulated Mode 6 Resonance Wavelength Shift versus strain induced by health interface.

4. Discussion

The presented results represent the very first stage of a study on the implementation of network fiber sensors in various special application fields, medical, research and industrial. This first stage consists mainly in creating the software packages of codes covering possible applications. The future research directions resulting from the mentioned study will be reported together with obtained experimental results in the papers to be published.

5. Conclusions

An analysis method of smart composite materials with optical fiber grating sensor embedded in its polymer matrix delamination process was developed. By incorporating the optical fiber grating sensor, the composite material is transformed into a smart one intended to be used in mechanical structures and/or parts construction and compatible with automatized systems. This compatibility is due to the use of the optical fiber grating sensor signal as input into a feedback loop of an automatization system. Based on presented simulation results improved design of smart composite materials with various applications in chemical industry including their operation as chemical sensors become possible.

6. Acknowledgements

This work was supported by the Core Program within the National Research Development and Innovation Plan 2022-2027, carried out with the support of MCID, project no. PN 23 05, the Romanian Ministry of Research, Innovation and Digitalization and a grant of the Ministry of Research, Innovation and digitalization, CNSC-UEFISCDI, project number PN- III-P4-PCE-2021-0585, within PNCDI III.

R E F E R E N C E S

[1]. *Aleksey Mironov, Andrejs Kovalovs, Andris Chate and Aleksejs Safonovs,* "Static Loads Influence on Modal Properties of the Composite Cylindrical Shells with Integrated Sensor Network", Sensors, **vol. 23,** no. 6, pp. 3327, 2023

[2]. *Yu Zhang, Yu Feng, Xiaobo Rui, Lixin Xu, Lei Qi, Zi Yang, Cong Hu, Peng Liu and Haijiang Zhang*, "Acoustic Source Localization in CFRP Composite Plate Based on Wave Velocity-Direction Function Fitting", Sensors, **vol. 23,** no. 6, 3052, 2023. DOI: 10.3390/s23063052

[3]. *B. Degamber, G.F. Fernando*, "Process Monitoring of Fiber-Reinforced Polymer Composites", MRS Bulletin, **vol. 27,** no. 5, 2002, pp. 370-380.

[4]. *K. Bocz, D. Simon, T. Bárány, G. Marosi*, "Key Role of Reinforcing Structures in the Flame-Retardant Performance of Self-Reinforced Polypropylene Composites", Polymers. **vol. 8**, 2016, pp. 289-301.

[5]. *K. Dobrovszky, F. Ronkay*, "Effects of Phase Inversion on Molding Shrinkage, Mechanical, and Burning Properties of Injection-molded PET/HDPE and PS/HDPE Polymer Blends", Polymer-Plastics Technology and Engineering, **vol. 56,** no.11, 2017, pp. 1147-1157.
[6]. *N. Malhotra, M. Kundabala, S. Acharya*, "Strategies to Overcome Polymerization Shrinkage - Materials and Techniques, A Review", Dental update, **vol. 37**, no. 2, 2010.
[7]. *J.K. Lee, J.K. Gillham*, "Evolution of properties with increasing cure of a thermosetting epoxy/aromatic amine system: physical ageing", J Appl Polym Sci, **vol. 90**, no.10, 2003, pp. 2665-2675.
[8]. *M.A. El-Sherif and J. Radhakrishnan*, "Advanced Composites with Embedded Fiber Optic Sensors for Smart Applications", Journal of reinforced Plastic and Composites, **vol.16**, no.2, 1997.
[9]. *J.H.L. Grave, M.L. Håheim, A.T. Echtermeyer*. "Measuring changing strain fields in composites with Distributed Fiber-Optic Sensing using the optical backscatter reflectometer", Composites Part B, **vol. 74**, 2015, pp. 138-146.
[10]. *S.W. James, R.P. Tatam*, "Optical fibre long-period grating sensors: characteristics and application", Meas Sci Technol, **vol. 14**, no. 5, 2003, R49–R61.
[11]. *A.M. Vengsarkar, P.J. Lemaire, J.B. Judkins, V. Bhatia, T. Erdogan, J.E. Sipe*, "Long-period fibre gratings as band-rejection filters", J Lightwave Technol, **vol. 14, no.** 1, 1996, pp. 58–65.
[12]. *T. Erdogan*, "Cladding-mode resonances in short- and long- period fiber grating filters", J Opt Soc Am A, **vol. 14,** no. 8, 1997, pp. 1760–1773.
[13]. *A. Groza, A. Surmeian, C. Diplasu, P. Chapon, D. Manaila-Maximean, and M. Ganciu, "*GD-OES and GD-MS investigations of the processes involved in the polymerization of polydimetylsiloxane in corona discharges. University Politehnica of Bucharest Scientific Bulletin-Series A-Applied Mathematics and Physics, **vol.** 73, no. 3, 2011, pp.133-140.
[14]. *A. Surmeian, D. Manaila-Maximean, B. Mihalcea, O. Stoican, B. Butoi, O. Danila, P. Dinca, I. Barbut, L. Tudor, A. Fazacas and E. Diplasu,* "GDOES and GDMS analytical systems, effective tools for characterization of conductive and nonconductive material surfaces. University Politehnica of Bucharest Scientific Bulletin-Series A-Applied Mathematics and Physics, **vol.** 77, no. 4, 2015, pp.273-280.
[15]. *T. Erdogan*, "Fiber grating spectra", J Lightwave Technol, **vol. 15,** no. 8, 1997, pp. 1277–1294.
[16]. *A.I. Kalachev, V. Pureur, D.N. Nikogosyan*, "Investigation of long-period fiber gratings induced by high-intensity femtosecond UV laser pulses", Opt Commun, **vol. 246**, no. 1-3, 2005, pp. 107–115.
[17]. *C.S. Cheung, S.M. Topliss, S.W. James, R.P. Tatam*, "Response of fibre optic long period gratings operating near the phase matching turning point to the deposition of nanostructured coatings", J Opt Soc Am B, **vol. 25,** no. 6, 2008, pp. 897–902.
[18]. *L. Zhang, W. Zhang, I. Bennion*, "In-Fiber Grating Optic Sensors" In: S. Yin, P.B. Ruffin, F.T.S. Yu editors, Fiber Optic Sensors. Second Edition. Boca Raton, FL: CRC Press, 2008, pp. 109–162.
[19]. *W.J. Bock, J. Chen, P. Mikulic, T. Eftimov*, "A novel fiber-optic tapered long-period grating sensor for pressure monitoring", IEEE T Instrum Meas, **vol. 56,** no. 4, 2007, pp. 1176–1180.
[20]. *S. Miclos, D. Savastru, R. Savastru, I. Lancranjan*, "Numerical analysis of Long Period Grating Fibre Sensor operational characteristics as embedded in polymer", Compos Struct, **vol. 183**, 2018, pp. 521-526, doi: http://dx.doi.org/10.1016/ j.compstruct.2017.04. 079, IDS No: FL9QV
[21]. *D. Savastru, S. Miclos, R. Savastru, I.Lancranjan*, "Study of thermo-mechanical characteristics of polymer composite ma-terials with embedded optical fibre", Compos Struct, **vol. 183**, 2018, pp. 682-687.

[22]. *D. Savastru, S. Miclos, R. Savastru, I.I. Lancranjan*, "Analysis of mechanical vibrations applied on a LPGFS smart composite polymer material", Compos Struct, **vol. 226**, art. no. 111243, 2019, pp. 1243-1250.

[23]. *S. Miclos, D. Savastru, R. Savastru, I.I. Lancranjan*, "Transverse mechanical stress and optical birefringence induced into single-mode optical fibre embedded in a smart polymer composite material", Compos Struct, **vol. 218**, 2019, pp. 15-26.

[24]. *E. Anemogiannis, E.N. Glytsis, T.K. Gaylord*, "Transmission characteristics of long period fiber gratings having arbitrary azimuthal/radial refractive index variations", J Lightwave Technol, **vol. 21,** no. 1, 2003, pp. 218–227.

[25]. *V. Bhatia, D.K. Campbell, D. Sherr, T.G. D'Alberto*, *N.A. Zabaronick, G.A.Ten Eyck, K.A. Murphy, R.O.Claus*, "Temperature-insensitive and strain-insensitive long-period grating sensors for smart structures", Optical Engineering, **vol. 36,** no. 7, 1997, pp. 1872-1875.

[26]. *K.O. Hill, B. Malo, F. Bilodeau, D.C. Johnson*, "Photosensitivity in optical fibers", Annu Rev Mater Sci, **vol. 23**, 1993, pp. 125–157.

[27]. *R. Falciai, A.G. Mignani, A. Vannini*, "Long period gratings as solution concentration sensors", Sensor Actuat B-Chem, **vol. 74,** no. 1-3, 2001, pp. 74–77.

[28]. *S. Korposh, R. Selyanchyn, W. Yasukochi, S.W. Lee, S.W. James, R.P. Tatam*, "Optical fiber long period grating with a nano-porous coating formed from silica nanoparticles for ammonia sensing in water", Mater Chem Phys, **vol. 133,** no. 2-3, 2012, pp. 784–792.

[29] *I. Lancranjan, D. Savastru, S. Miclos, A. Popescu*, "Numerical simulation of a DFB-fiber laser sensor (II) – theoretical analysis of an acoustic sensor", J. Optoelectron. Adv. Mater. **vol. 12**, no. 12, 2010, pp.2456÷2461, IDS No.704HW

[30] *S. Miclos, D. Savastru, I. Lancranjan*, "Numerical simulation of a fiber laser bending sensitivity", Rom.Rep Phys., **vol.62**, no.3, 2010, pp.519-527, IDS No.720HU

[31]. *L. Zeng and R. Olsson,* "Buckling-induced delamination analysis of composite laminates with soft inclusion", FOI-R--0412—SE, Technical report, Stockholm (Sweden), Swedish Defence Research Agency; 2002, pp. 34, ISSN 1650-1942.